Potential of Marine Sponge-Associated Fungi (*Callyspongia* sp.) as Textile Dye Biodegradation Agents

Erlita Dwi Octaviani[1,2], Agus Trianto[1,2]*, Ocky Karna Radjasa[3], Bambang Yulianto[1], Agus Sabdono[1], Erin M. Cauley[4]

[1]Department of Marine Science, Faculty of Fisheries and Marine Science, Universitas Diponegoro
[2]Marine Natural Product Laboratory, Centre for Research and Services, Universitas Diponegoro
Jl. Prof. Jacub Rais, Tembalang, Semarang Jawa Tengah 50275 Indonesia
[3]National Research and Innovation Agency
Gedung B.J. Habibie Jl. M.H. Thamrin No. 8, Jakarta Pusat 10340, Indonesia
[4]California State University Dominguez Hills
1000 E Victoria St, Carson, CA 90747 United States
Email: agustrianto@lecturer.undip.ac.id

Abstract

Textile industries generate large volumes of wastewater containing synthetic dyes such as azo, naphthol, and rhodamine B, which are highly resistant to degradation and pose significant environmental risks when discharged into aquatic ecosystems. These dyes can be toxic to aquatic life, disrupt food chains, and cause long-term pollution. This study aimed to evaluate the biodegradation potential of marine fungi isolated from the sponge Callyspongia sp. as a natural and eco-friendly solution for textile dye removal. Two fungal isolates, RA.S12.1 and RA.S12.2, were tested on solid and liquid media with 200 ppm dye concentrations. Isolation involved collecting sponges from marine environments and culturing them on selective media to obtain fungal colonies. Decolorization was assessed through qualitative observations (changes in growth zone color) and quantitative analyses using UV-Vis spectrophotometry to measure absorbance reductions at specific wavelengths, as well as CMYK color measurements to quantify objective color intensity changes. Results indicated that isolate RA.S12.2 achieved the highest decolorization percentage of 64.8% for Azo Mordant Black 17 after 7 days of incubation, while RA.S12.1 reached only 30.1%. Molecular identification via ITS rDNA gene sequencing confirmed both isolates as Penicillium citrinum with 100% homology. These findings suggest that marine-derived P. citrinum holds strong potential as a bioremediation agent for textile dye degradation, offering an environmentally friendly alternative for wastewater treatment in coastal and marine areas impacted by industrial pollution. This approach could provide a sustainable alternative to conventional chemical methods, with broader applications in mitigating global aquatic pollution. Further research is needed to optimize conditions and test at an industrial scale.

Keywords*: Textile Dyes; Decolorization; Marine Fungi; Penicillium citrinum; Environmental biotechnology*

Introduction

Indonesia is one of the countries with rapid industrial growth in the ASEAN region. However, several industries are sources of heavy metal pollution such as manganese (Mn), copper (Cu), zinc (Zn), cobalt (Co), chromium (Cr), Iron (Fe), lead (Pb), and polycyclic aromatic hydrocarbons (PAHs) (Haris *et al.*, 2024; Shintianata *et al.,* 2024; Sukardi *et al.*, 2024). However, the increased use of synthetic dyes in textile processing leads to substantial liquid waste discharge into aquatic environments. Azo, naphthol, and rhodamine B dyes are widely used due to their chemical stability and coloration efficiency, yet these compounds are persistent, toxic, and often carcinogenic, posing serious environmental and health risks when released into natural waters (Schmidt *et al*., 2019).

Conventional physical and chemical wastewater treatment methods are generally capable of reducing dye concentration; however, they are costly, require large amounts of chemicals, and generate secondary sludge that must be further managed (Madalosso *et al*., 2022). For this reason, environmentally friendly alternatives such as biodegradation have gained increasing attention. Biodegradation utilizes microorganisms—particularly fungi and bacteria—to convert hazardous pollutants into less harmful or harmless substances (Srinivasan and Sadasivam, 2021).

Fungi possess diverse enzymatic systems that enable them to degrade complex organic molecules, including xenobiotic dyes (Hossen *et al*., 2019). Marine fungi are especially promising due to their adaptive capabilities in extreme environments, such

*) Corresponding author

https://ejournal.undip.ac.id/index.php/ijms
DOI: 10.14710/ik.ijms.30.4.597-612
Received : 06-05-2025
Accepted : 07-11-2025

as high salinity and variable nutrient conditions. Marine sponges act as filter feeders and host diverse microbial symbionts that obtain and process dissolved organic materials from seawater (Bahry *et al*., 2021). These sponge-associated organisms are known to produce extracellular enzymes, such as laccase, which can oxidize phenolic and non-phenolic compounds and potentially mineralize dye molecules into non-toxic forms (Ayilara *et al*., 2020; Maharsiwi *et al*., 2020).

Despite growing interest in microbial dye degradation, studies focusing on fungi from marine sponge associations remain limited. Prior research highlights their potential enzymatic activity and ecological importance (Trianto *et al*., 2023), yet few investigations have systematically evaluated their ability to decolorize multiple textile dyes or quantitatively assessed degradation efficiency. Therefore, the present study aims to explore the biodegradation potential of fungal isolates obtained from the sponge *Callyspongia* sp. against several classes of textile dyes. Specifically, this research evaluates their decolorization performance through qualitative and quantitative methods and further identifies the isolates using molecular markers (ITS1 and ITS4). The outcomes are expected to contribute to the development of sustainable and marine-based bioremediation strategies for textile pollutant mitigation.

Materials and Methods

Isolate rejuvenation

Marine sponge samples (*Callyspongia* sp.) were collected from coastal waters, with sampling conducted carefully to avoid damage to sponge habitats in accordance with ethical marine conservation considerations. Sponge fragments were transported in sterile seawater to preserve natural salinity conditions. The fungal isolates stored in glycerol stocks were rejuvenated on Potato Dextrose Agar (PDA) and incubated for 7 × 24 h to obtain active cultures, following the method of Alam *et al*. (2022).

Fungi characterization

Macroscopic characterization included observations of colony morphology, color, texture, margins, elevation, and exudate presence. Microscopic characterization—such as spore morphology, hyphal structure, and conidiophore patterns—was carried out using the slide culture technique described by Sibero *et al*. (2018). Morphological descriptions were compared with the MycoBank database for preliminary identification.

Qualitative dye degradation

The qualitative degradation test was conducted on PDA media enriched with Azo Mordant Black 17, Azo Dark Blue, Rhodamine B, and Naphthol Brown at concentrations of 200 ppm. The assay followed the procedures adapted from Lalnunhlimi and Veenagayathri (2016). Fungal isolates were inoculated on the media and incubated for five days at ambient temperature to simulate coastal water conditions. Clear zones appearing around colonies on days 3 and 5 were used as indicators of decolorization potential.

UV decolorization analysis - spectrophotometer

The determination of the decolorization of these three dyes was performed using a UN/Vis spectrophotometer. Measurements were carried out once every day for five days by taking sufficient culture medium to be centrifuged at 4000 rpm for 30 min. The supernatant was filtered through Whatman paper, and the absorbance was measured using a spectrophotometer (Caguiat *et al*., 2024). The absorption value was determined by comparing the concentration of the culture medium before and after the absorption. The dye concentration was determined using a visible spectrophotometer at a maximum wavelength of 520 nm. Each treatment was repeated three times. Controls were prepared in the same way, without the addition of the fungal suspension. For each treatment, the percentage of decolorization was calculated to determine the decrease in the intensity of the dye in the medium that had been given textile dyes. The decolorization percentage was determined using the following formula:

$$\text{Decolorization}\,(\%) = \frac{\text{Absorbance before treatment} - \text{Absorbance after treatment}}{\text{Absorbance before treatment}} \times 100\%$$

CMYK color analysis

To complement spectrophotometric measurements, CMYK analysis was employed to determine visual color changes. Images were processed using Adobe Photoshop CS6, and values of cyan, magenta, yellow, and key (black) were recorded before and after fungal treatment. This method was used to support visual quantification of decolorization as applied in colorimetric assessment studies (Phuangsaijai *et al.*, 2021).

Molecular identification of fungi

Molecular identification of fungi was carried out in several stages, including DNA extraction, DNA

amplification by PCR, electrophoresis and visualization of PCR results, DNA sequencing, and phylogenetic analysis. The steps involved in the molecular identification of fungi are as follows:

DNA extraction

DNA extraction was carried out using the Zymo DNA Extraction Kit for fungi, following the protocol provided in the kit. Pure fungal isolates were grown on agar medium for 7 days for DNA extraction.

DNA amplification by PCR

Amplification was carried out using an Internal Transcribed Spacer (ITS) as a primer for fungal barcoding by polymerase chain reaction (PCR). There are components of the PCR mixture including 12.5 L GoTaq Green Master mix from Promega Corporation, 1 L from ITS1 (5′-TCC GTA GGT GAA CCT GCG G-3) as forward primer, 1 L from ITS4 (5′-TCC TCC GCT TAT TGA TAT GC-3) as reverse primer from Macrogen, 9.5 L ddH2O solution and 1 L DNA template (Sibero *et al*., 2018).

The steps in PCR are denaturation at a temperature of 95°C for 1 min; 34 cycles of denaturation at 95°C for 3 min, annealing at 56.1°C for 1 min, elongation at 72°C for 1 min; the last elongation at 72°C for 7 min and cooling at 4°C (Trianto *et al*., 2020). Electrophoresis and PCR Results Visualization:The quality of PCR products was checked by electrophoresis with Tris base buffer, acetic acid and EDTA (TAE) 1X. Agarose gel was prepared by dissolving 1 g of agarose in 100 mL of TAE 1X, and then fungying using fungi and an electrophoresis comb. After cooling, the gel was placed in a tank filled with TAE 1X. A total of 5 L of the PCR product was inserted into a 1% agarose well, and 3 L of DNA leader was inserted into one agarose well. A current of 100 Volts was then flowed from the negative pole to the positive pole for 30 min, taken, and used for the staining stage. Agarose was immersed in an ethidium bromide (Etbr) dye solution for 30 min. Agarose was then placed into the gel documentation and irradiated with a UV lamp. Samples containing DNA bands were sent for sequencing. The sequencing stage was carried out in 1st Base Malaysia (Sibero *et al*., 2018).

DNA Sequencing and Phylogenic Analysis: The obtained sequences were processed using MEGA X software. Sequences received from 1st Base Malaysia were then matched with the GenBank database to determine the fungal species. This stage uses the Basic Local Alignment Search Tool (BLAST) found in https://blast.ncbi.nlm.nih.gov/Blast.cgi. A phylo-genetic tree was constructed by aligning all sequences and their comparison sequences. Algorithm analysis was performed using neighbor-joining (NJ) and testing was performed with a bootstrap value of 1000 times.

Result and Discussion

Microscopic and macroscopic characterization

All sponge-associated fungal isolates, up to two, were identified by colonization characterization, observing the fungi macroscopically (colonial) and microscopically. The overall fungal characteristics are presented in Table 1 and 2.

The fungal isolates were identified using macroscopic and microscopic observations of the colonies. Based on the results of fungal isolation from marine fungal isolates, two isolates were active and could grow on PDA medium. Macroscopic observation of isolated RA S12.2: had a characteristic green color with white colonies, white mycelium, a brown color behind the colony, and no exudates. The two isolates had the same characteristics and morphology as those of the genus Penicillium. This is in accordance with the theory of Barnett and Hunter (1972) that the microscopic characteristic of the Penicillium fungus is that the conidia have thick walls, the young conidia strands are at the proximal base of the strand. conidiophores branched circularly either single or double, conidia produced at the end in a series, round in shape, numerous and brightly colored

The fungal isolates in this study were identified using macroscopic and microscopic observations. Based on the results of fungal isolation from marine fungal isolates, two isolates were active and could grow on Potato Dextrose Agar (PDA) media. Based on macroscopic observations, isolate RA.S12.1 was characterized by green colony color, white mycelium, white colony turning color, and no exudates. Macroscopic observation of isolate RA S12.2 revealed a characteristic green color with white colonies and white mycelium, and the color behind the colony was brown with no exudates (Figure 1).

After identification, the two isolates were found to have the same morphological characteristics. Microscopic observations revealed that the conidia were round, the hyphae were insulated, and conidiophores were present. The two isolates had the same characteristics and morphology as those of the genus Penicillium. This is in accordance with the theory of Zakariya *et al.* (2022), who stated that the microscopic characterization of the Penicillium fungus shows that the conidia have thick walls and that the young conidia strands are on the proximal base of the strands. Conidiophores are circularly branched, either single or double, and conidia are produced at the end

Table 1. Macroscopic Characterization Results

Isolate Code	Colony Color	mycelium	*Exudates*	*reverse*
RA.S12.1	Green	White	There is not any	White
RA.S12.2	Green-white	White	There is not any	Chocolate

Table 2. Microscopic Characterization Results

Isolated Code	Conidiophores	Conidia	*Fialid*	*hyphae*
RA.S12.1	Monothematic	Round	there is	bulkhead
RA.S12.2	Monote Matous	Round	there is	bulkhead

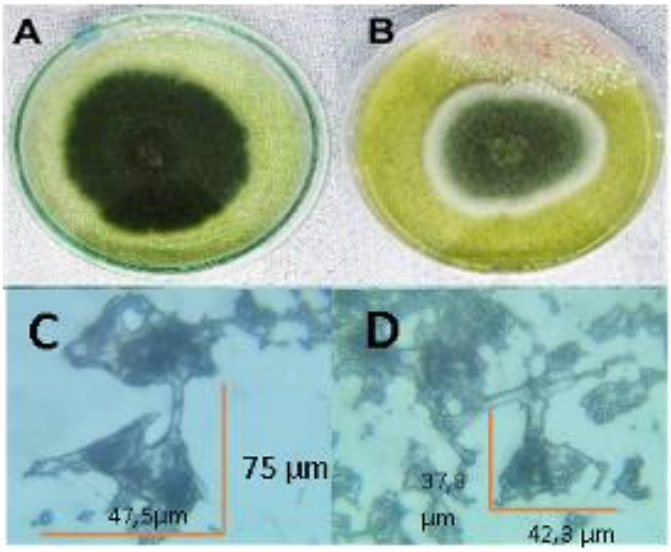

Figure 1. Mold colonies and Microscopy Morphology of molds. A: Macroscopic mold isolate RA.S12.1 B: Macroscopic mold isolate RA.S12.2 C: Microscopic mold isolate RA.S12.1 D: Microscopic mold isolate RA.S12.2.

in a series, are round in shape, numerous, and brightly colored (Géry *et al*., 2021). Based on the identification by Torres-Garcia, Gene and Garcia (2022), Penicillium colonies were initially white, then changed to turquoise, greenish gray, olive gray, sometimes yellow or reddish-red, and the reverse color was usually pale yellow, while microscopic forms of Penicillium fungus have hyaline hyphae, conidia are round, and unicellular, and have a group of phialides.

Qualitative dye degradation test

The qualitative dye degradation assay showed that both fungal isolates, RA.S12.1 and RA.S12.2, were capable of decolorizing textile dyes on PDA media at a concentration of 200 ppm. Clear decolorization zones appeared around the colonies as early as day 3 and became more pronounced by day 5, which is commonly used as a primary indicator of dye degradation ability on solid media (Lalnunhlimi and Veenagayathri, 2016). RA.S12.2 produced larger and more uniform clear zones on Azo Mordant Black 17 and Azo Dark Blue, whereas RA.S12.1 showed a stronger visible activity on Naphthol Brown. These differences may reflect variations in enzymatic affinity and dye molecular structures, as marine fungi possess extracellular enzymes, such as laccases, capable of degrading phenolic and non-phenolic substrates (Maharsiwi *et al*., 2020; De Paula *et al*., 2022).The results of the degradation tests for various textile dyes are shown in Figure 2–5.

The formation of clear zones is relevant in the context of marine pollution because azo and naphthol dyes are persistent, toxic, and resistant to degradation in aquatic environments (Schmidt *et al*. 2019). The ability of *Penicillium citrinum* to initiate chromophore cleavage suggests its potential application in coastal wastewater treatments, particularly as sponge-associated fungi are adapted to saline environments and are exposed to diverse organic compounds (Bahry *et al*., 2021). Although solid media do not fully replicate marine conditions, such as fluctuating salinity and pH, this initial qualitative screening

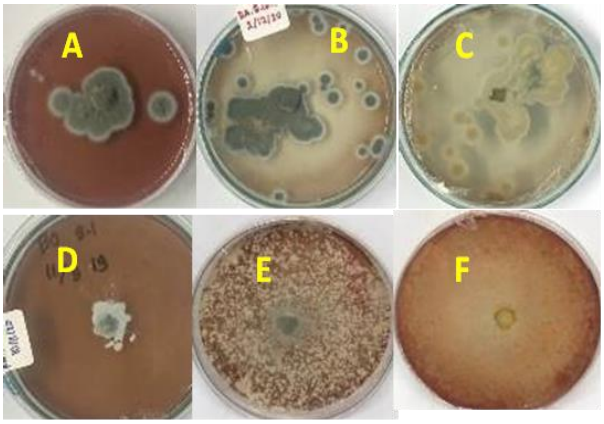

Figure 2. Results of the Qualitative Degradation Test of Chocolate Naphthol A: Isolate of RA. S12.1 1st day no degradation occurred. B: Isolate of RA mold. S12.1 on the 3rd day, a clear zone began to appear. C: Isolated RA mold. S12.1 5th day the color starts to degrade. D: Isolated mold RA.S12.2. the 1st day there is no degradation. E: RA mold isolated. S12.2 on the 3rd day there has been no degradation. F: Isolated RA mold. On the 3rd day of S12.2, the clear zone began to appear.

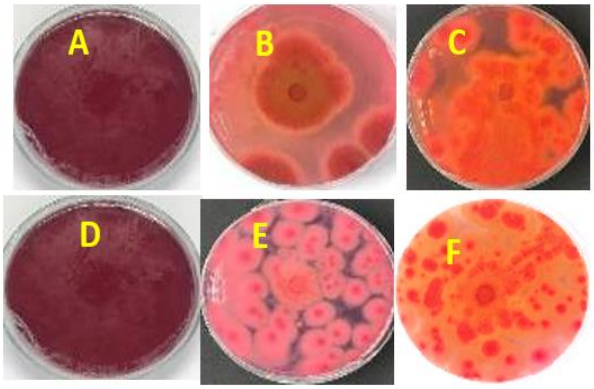

Figure 3. Results of Qualitative Degradation. Test of Rhodamine B. A: Isolate of RA.ST12.1 1st day no degradation occurred B: Isolate of RA mold. S12.1 on the 3rd day, a clear zone began to appear. C: Isolated RA mold. ST12.1 5th day the color starts to degrade. D: Isolated mold RA.S12.2 the 1st day there is no degradation. E: RA mold isolated. S12.2 on the 3rd day a clear zone was seen. F: Isolated RA mold. S12.2 5th day the color starts to degrade.

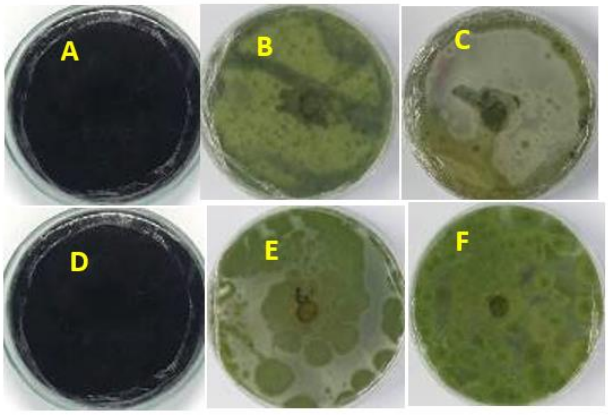

Figure 4. Results of Qualitative Degradation. Test for Azo Mordan Black 17. A: Isolate of RA.ST12.1 1st day no degradation occurred. B: Isolate of RA mold. S12.1 on the 3rd day, a clear zone began to appear. C: Isolated RA mold. S12.1 5th day the color starts to degrade. D: Isolated mold RA.S12.2. the 1st day there is no degradation. E: RA mold isolated. S12.2 on the 3rd day a clear zone was seen. F: Isolated RA mold. S12.2 5th day the color starts to degrade and disappear.

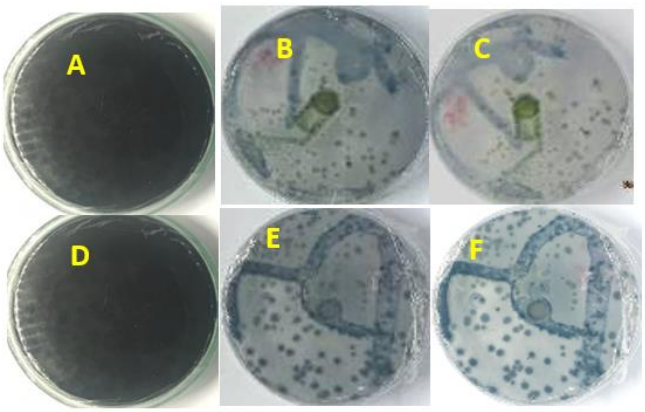

Figure 5. Azo Dark Blue Qualitative Degradation. Test Result. A: Isolated RA mold. S12.1 1st day no degradation occurred. B: Isolated of RA mold. S12.1 on the 3rd day, a clear zone began to appear. C: Isolate RA mold. S12.1 5th day the color starts to degrade. D: Isolated mold RA.S12.2. the 1st day there is no degradation. E: RA mold isolate. S12.2 on the 3rd day a clear zone was seen. F: Isolated RA mold. S12.2 5th day the color starts to degrade.

provides evidence that *P. citrinum* has promising dye-degrading potential, especially against azo-based dyes.

The degradation test can be observed based on the decrease in color intensity in the media, which can be used as an early indicator of the dye degradation process. This biodegradation research used four kinds of dyes, namely Naphthol brown, Rhodamine B, Azo Mordan Black 17, and Azo Dark Blue. The biodegradation study of the four dyes started with an agar plate containing PDA and the four dyes as a growth medium for fungi. The aim was to prove the extent to which marine fungi can degrade the four dyes. Observations were made on days 0, 3, and 5 to determine the decolorization ability of each fungal isolate against the four dyes. Based on Figure 3, the results of the qualitative degradation test showed a clear decolorization zone around the media, whose size varied depending on the type of fungal isolate used. The degradation results of the RA.S12.1 isolate were more visible on naphthol brown dye than on rhodamine B, Mordan Black 17, and Azo Dark Blue dyes. This indicates that isolate RA.S12.1 began to show a clear zone on the 3rd day of incubation. On the 5th day, the clear zone of RA.S12.2, isolated around the fungal colony, expanded, accompanied by the expansion of fungal growth.

The degradation results of the RA.S12.2 isolate were more pronounced for Mordan Black 17, Rhodamine B, and Azo Dark Blue dyes than for brown naphthol dyes. This occurred because the RA.S12.2 isolate on the 3rd day started to show a clear zone and the color started to fade. It was observed that there was binding of dye by the fungal colony, causing the dye available on the media to be clear. The results of the degradation of the two isolates indicated that isolate RA.S.12.2 has greater potential as a dye-degrading fungus. According to Alam *et al*. (2022), the formation of a clearing or fading zone on the medium is an early indication that the fungal isolate has potential as a dye-degrading fungus.

The high use of dyes in certain industrial activities increases the number of pollutants in the generated wastewater. Textile dyes are non-biodegradable organic pollutants. Textile dyes include naphthol, azo, and rhodamine B dyes. These naphthol dyes are still widely used in households. According to Lellis *et al*. (2019), naphthol dyes have adverse effects on human health, with the main risk being eye and respiratory tract irritation. The chemical structures of the naphthol dyes are presented in Figure 8.

Azo dyes are the most widely used chemicals in the industry and food, one of which is Mordan Black17. However, the use of azo dyes causes environmental pollution. About 10-15% of the dye used remains and is wasted in the environment. Azo dyes are organic compounds because the azo functional group combined with an aromatic ring is carcinogenic, soluble in water, and easily absorbed by the human body, making it difficult to decompose (He *et al*., 2018). The compounds present in these dyes are toxic and carcinogenic.

Rhodamine B is a dye in the form of a green or red-purple crystalline powder that is odorless and easily soluble in a bright red fluorinated solution, and is used as a dye for textiles, paints, and paper. Rhodamine B can irritate the respiratory tract and cause cancer with continuous use (Danish *et al*., 2017). According to Jing *et al*. (2022), rhodamine B is

harmful to health because it contains chlorine (Cl). A similar amount of Chlorine (Cl) is a halogen compound that is dangerous and reactive. Chlorine (Cl) in the body causes this compound to fight. It can be stabilized in the body, even when combined with other compounds. Its presence is highly toxic to the body. Other compounds that are bound no longer function properly because the body's performance is no longer optimal. The benefits of using this quantitative degradation method are that it is easy to observe every day, and you will see the difference from day 0 to day 5 can be observed.

UV decolorization analysis – spectrophotometer

In this study, a quantitative analysis of azo textile dye decolorization was performed by measuring the absorbance at 520 nm. The decrease in absorbance of the medium with various textile dyes at a concentration of 200 ppm using the two fungal isolates is presented in Table 3.

The decolorization of textile dyes can be determined from the percentage decolorization. The percentage of decolorization was expressed as the percentage decrease in the intensity of brown naphthol, azo Moerdan Black 17, and azo Dark Blue textile dyes and their concentrations by marine fungal isolates. The Uv-Vis spectrophotometric analysis supported the qualitative observations. RA.S12.2 achieved the highest decolorization percentage of 64.8% for Azo Mordant Black 17, whereas RA.S12.1 showed 30.1% under the same conditions. The reduction in absorbance reflects the breakdown of chromophores, in accordance with previous findings that fungal metabolism contributes to dye mineralization (Cemalgil *et al*., 2021; Alam *et al*., 2022). Under static conditions, improved decolorization is expected because of enhanced oxygen transfer and biomass interaction (Ahmed *et al*., 2022).

The decolorization of textile dyes can be observed from the percentage decolorization. The percentage of decolorization was expressed as the percentage decrease in the intensity of brown naphthol, azo Moerdan Black 17, and azo Dark Blue textile dyes by marine fungal isolates and their concentrations. The decolorization power was calculated to determine the decolorization ability of each isolate when treated with different types of textile dyes. Based on Table 3 The highest decolorization percentage was 28.9% for the textile dye Mordan Black 17 by isolating RA.S12.2, whereas the lowest decolorization percentage was 59.3% for the textile dye Rhodamine B by isolating RA. S12.1. According to Ahmed *et al*. (2022), under static conditions, microbial growth will benefit more and achieve better decolorization because this condition is associated with increased transfer of biomass and oxygen between cells. At a concentration of textile dyes at 200 ppm, all isolates were able to grow, indicating that textile dyes could be the sole carbon source for the growth of each fungal isolate on Cemalgil *et al*. (2021) media, where textile dyes containing hydroxyl groups were used as the sole source of growth. is the only source of nutrition for the organism.

According to De Paula *et al*. (2022), fungi tend to use only a single carbon source. If there are two carbons with different molecular complexities, growth will show a diauxic pattern. In diauxic growth, a carbon source that is more easily metabolized by the cell is used first. After the carbon source is depleted, fungi use other, more complex carbon sources. According to Cemalgil *et al*. (2021), the environment can support the growth and activity of several fungal groups. It is hoped that some of these fungi can degrade textile dyes because of the similarity in the structure of the parent compound and its intermediate products, which means that there are similar enzymes that play a role in this process.

CMYK decolorization analysis

The analysis for determining the decolorization of these three dyes used Adobe Photoshop CMYK (Cyan Magenta Yellow Black) to determine the percentage of color decolorization before and after degradation. The results of the percentage of CMYK decolorization are presented in Table 4 and 5 Decolorization of CMYK.

Table 3. Decolorization Percentage by UV-Spectrophotometry

Coloring type	Decolorization percentage (%)		
	Control	Isolate 1	Isolate 2
Naphthol chocolate	87.3	35.3	40.2
Rhodamine B	89.4	59.3	54.0
Azo Mordan Black 17	93.7	28.9	25.3
Azo Dark Blue	88.7	29.8	28.9

Table 4. Decolorization CMYK Control.

Coloring type	Decolorization percentage (%)							
	C		M		Y		K	
	S.12.1	S.12.2	S.12.1	S.12.2	S.12.1	S.12.2	S.12.1	S.12.2
Naphthol Brown	36	36	52	85	85	45	45	85
Rhodamin B	30	30	83	83	49	49	49	49
Azo Mordan Black 17	63	63	52	52	51	51	100	100
Azo Dark Blue	64	64	50	50	48	48	70	70

Table 5. Decolorization CMYK Isolate RA.S12.1 and RA.S12.2.

Coloring type	Decolorization percentage (%)							
	C		M		Y		K	
	S.12.1	S.12.2	S.12.1	S.12.2	S.12.1	S.12.2	S.12.1	S.12.2
Naphthol Brown	34	35	36	38	74	78	26	24
Rhodamin B	24	22	52	56	27	29	13	12
Azo Mordan Black 17	43	45	41	41	59	61	32	30
Azo Dark Blue	56	58	46	40	44	47	32	34

Color decolorization was determined using Adobe Photoshop CMYK to calculate the percentage of decolorization. CMYK is a subtractive color used in combination with several primary colors. This color decolorization was determined using the Adobe Photoshop CS6 application by inputting an image or image and then selecting five sampling points on the color of the image. The lowest percentage was for Rhodamine B, with C, M, Y, and K values of 26.7%, 32.5%, 40.8%, and 75.5 %, respectively. The percentage decrease in color intensity in isolate RA.S12.2 Mordan Black 17 was C 31.7%, M 21.2%, Y -15.7%, and K 68%.

The lowest percentage was observed in naphthol brown, with C, M, Y, and K values of 5.6%, 30.8%, 12.9%, and 42.2 %, respectively. This is reminiscent of the formation of subtractive colors, which states that if the three primary color components in the CMYK color have the same value, namely 100%, then black will be formed, so that the other colors will be worth 0. If the minimum value of the CMYK vector data is not the same as the pure color, the value of the black color is the minimum value.

CMYK analysis was used as an additional verification technique. The values of cyan, magenta, yellow, and key decreased after fungal treatment, confirming visual decolorization and supporting the usability of color-based quantification in textile dye analysis (Phuangsaijai *et al*., 2021). The concordance between the UV-Vis and CMYK measurements strengthens the reliability of the results.

Dye decolorization was determined using Adobe Photoshop CMYK (Cyan Magenta Yellow Key or blue, pink, yellow, and black colors) to determine the percentage of color decolorization. CMYK is a subtractive color, which is a color used in combination with several primary colors (Phuangsaijai *et al.*, 2021). CMYK decolorization was performed using Adobe Photoshop CS6 by inputting an image or image and then selecting five sampling points on the color of the image. The result of the highest percentage decrease in color intensity in RA.S12.1 isolate was in brown naphthol dye, with C values of 2.8%, 26.9%, 8.2%, and 46.7 %, respectively. The brown component consists of the primary colors of magenta, yellow, and key. The lowest percentage was for Rhodamine B, with a C value of 26.7%, M of 32.5%, Y of 40.8%, and K of 75.5%. The percentage decrease in color intensity in the isolate RA.S12.2 Mordan Black 17 was C 31.7%, M 21.2%, Y -15.7%, and K 68%. The lowest percentage was observed in naphthol brown with C, M, Y, and K values of 5.6%, 30.8%, 12.9%, and 42.2 %, respectively.

Cai-yin *et al.* (2017), said that the CMYK value can be obtained by operating subtraction pure color values with known color component values. If the smallest value of the CMYK color formed is 1 (pure color), then it can be ascertained that pure black will be formed, and the other colors will be 0 (no color). This is reminiscent of the formation of subtractive colors, which states that if the three primary color components in the CMYK color have the same value, namely 100%, then black will be formed so that the other colors will be worth 0. If the minimum value of the CMYK vector data is not the same as the pure

color, then the value of the black color formed is the minimum value. The advantages of using the CMYK method are that it is easy to use, obtains a percentage of color reduction, and is inexpensive. However, the drawback of this method is that the percentage value for color decolorization is not yet accurate because no studies have used this method yet.

Molecular identification of fungi

Potential isolates amplified by PCR were characterized by the formation of a single band of fungal DNA. The gene amplification results were used for further identification of the species. The isolate RA.S12.1 showed the location of the band at 580 bp, while isolate RA.S12.2 showed the location of the band at 570 bp obtained from BLAST Homology tracing. The results of DNA visualization of fungal isolates RA.S12.1 and RA.S12.2 are shown in Figure 6.

The results of DNA visualization of the fungal isolates showed that the location of the band was between 550 bp and continued with homology BLAST analysis. The results obtained were isolates RA.S12.1 and RA.S12.2, which showed a 100% close kinship level with *Penicillium citrinum* (Acc Number 121224.1) and comparison of outgroup sequences with *Tricodherma alni* (Acc Number KX632S24.1). The results of base pair data processing for the manufacture of phylogenetic trees showed that there was clustering of marine fungi isolates with other organisms closest to the furthest kinship levels. The level of kinship in fungal isolates RA.S12.1 and RA.S12.2 showed a very close relationship with *Penicillium citrinum*, as shown in Figure 7.

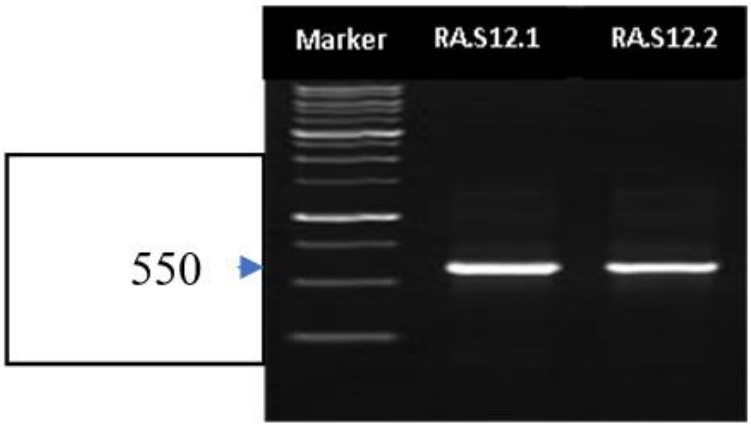

Figure 6. The results of DNA visualization of molds RA.S12.1 and RA.S12.2 showed that the location of the band was 550 bp.

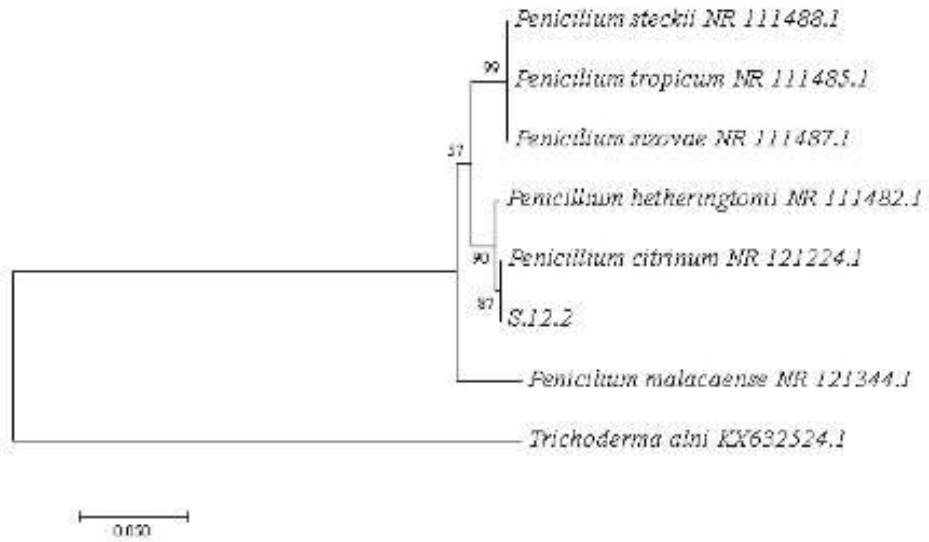

Figure 7. Phylogenetic Tree of Mold Isolates RA.S12.1 and RA.S12.2 which shows a very close relationship with *Pencilium citrinum.*

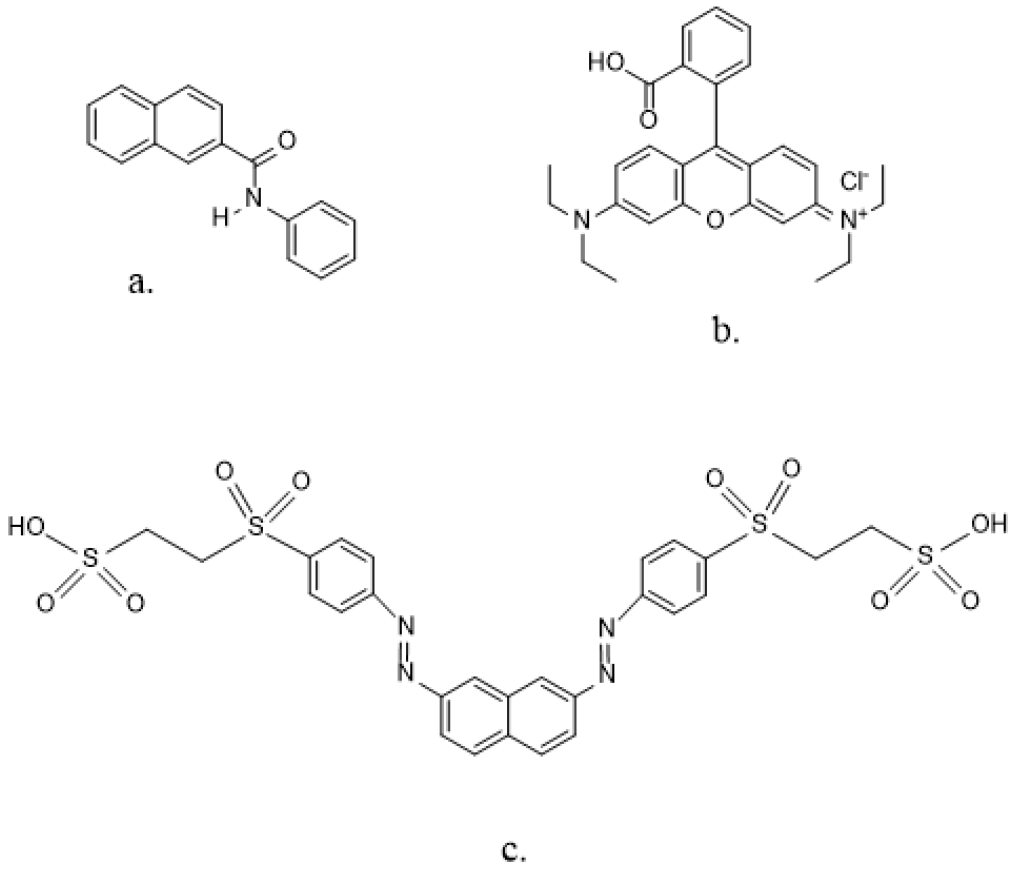

Figure 8. Chemical Structure a. Naphthol (Jing *et al.,* 2022)., b. of Rhodamine B (Tsamo *et al.,* 2020). C. Azo Mordan Black 17 (Franciscon *et al*., 2012)

Molecular identification of fungi was performed for two active isolates of marine fungi with isolate codes RA.S12.1 and RA.S12.2, which formed inhibition zones in screening and degradation tests of textile dyes. Based on the results obtained from the Homology BLAST search, it was found that isolates RA.S12.1 and RA.S12.2 showed a 100% close kinship level with *Penicillium citrinum*, as well as a comparison of outgroup sequences with *Tricodherma alni.* Two sequences with an E-value of 0 were considered identical.

Base pair data processing for phylogenetic tree construction showed that marine fungal isolates were grouped with other fungi closest to the furthest kinship levels. Phylogenetics, the taxonomic classification of organisms, is central to biological evolution. The outgroup used is *Tricodherma alni*. because it is a species that is not closely related to the fungi isolates RA.S.12.1 and RA.S12.2.

The neighbor-joining method was used to construct phylogenetic trees because it is accurate for constructing phylogenetic trees with short branches. Neighbor-joining selects sequences that, when combined, provide the best estimate of the length of the closest branch, thus reflecting the actual distance between the sequences. This phylogenetic tree was constructed using the neighbor-joining method and bootstrap analysis (1000 repetitions), resulting in a value of 86%, which means that these five isolate sequences were significantly different from the outgroup because they had different base pair sequences (Chin *et al*., 2021).

Molecular identification of fungi was performed for two active isolates of marine fungi with isolate codes RA.S12.1 and RA.S12.2, which formed inhibition zones in screening and degradation tests of textile dyes. Based on the results obtained from the Homology BLAST search, it was found that isolates RA.S12.1 and RA.S12.2 showed a 100% close kinship level with *Penicillium citrinum* (Acc Number 121224.1) and a comparison of outgroup sequences with *Tricodherma alni* (Acc Number KX632S24. 1).

The results of the data analysis can be categorized as very good because the percentage of

similarity is very high (*i.e.,* > 97%), and the value of e is 0. Isolates with a similarity percentage > 97% can represent the same species (Hyde *et al*., 2019), which is an estimated value that provides a statistically significant measure between the two sequences. A greater e value indicates that the level of homology between the two sequences decreases; however, if the e value becomes smaller than, the level of homology between the two sequences increases. Two sequences with an e-value of 0 can be considered identical (Trianto *et al*., 2020).

Base pair data processing for phylogenetic tree construction showed that marine fungi isolate clustered with other fungi closest to the furthest kinship levels. Phylogenetics can be defined as the taxonomic classification of organisms and is central to biological evolution. The phylogenetic tree constructed in this study was used to determine the evolutionary distance between certain species to determine the relationship between marine fungal isolates. This relationship is illustrated in Figure 9. The degree of kinship between the fungal isolates RA.S.12.1 and RA.S12.2 was very close to that of *Penicillium citrinum*. The outgroup used was *Tricodherma alni* (KX632S24.1). because it is a species that is not closely related to the fungi isolates RA.S.12.1 and RA.S12.2

The neighbor-joining method was used in the construction of phylogenetic trees because it is accurate for the construction of phylogenetic trees with short branches. Neighbor-joining selects sequences that, when combined, provide the best estimate of the length of the closest branch, thus reflecting the actual distance between sequences. Neighbor-joining is also used more often because the calculation process is relatively fast and easy. The bootstrap value indicates whether the analysis of the model dataset test was good or not. This validates the arrangement of branches to predict the resampled rate in the construction of branches and twigs of phylogenetic trees (Hong *et al*., 2021). The genetic distance in the phylogenetic tree showed a value of 0.050, which means that there was a difference of five bases in every 100 bases of each sequence. Phylogenetic tree construction using the neighbor-joining method and bootstrap analysis (1000 repetitions) resulted in a value of 86%, indicating that these five isolate sequences were significantly different from the outgroup because of their different base pair sequences (Riesco *et al*., 2018).

Conclusion

This study showed that marine sponge-associated *Penicillium citrinum* isolates RA.S12.1 and RA.S12.2 were able to degrade synthetic textile dyes, with RA.S12.2 achieving the highest decolorization efficiency of 64.8% on Azo Mordant Black 17. Qualitative clear zone formation and quantitative UV-Vis and CMYK analyses confirmed their dye-degrading capabilities. These findings indicate that p-derived fungi have potential as environmentally friendly bioremediation agents for textile wastewater, especially in coastal regions where dye discharge threatens marine ecosystems. *P. citrinum* could be considered as a complementary treatment strategy for coastal textile industries to reduce dye concentration before effluent enters seawater. Future research should focus on testing performance under real marine conditions, including salinity and pH fluctuations, and scaling applications through pilot bioreactors using mixed-dye wastewater. Overall, this work highlights the promise of marine fungi as nature-based solutions supporting sustainable wastewater management and coastal environmental protection.

Acknowledgement

This work was supported by grants from the DRPM Ministry of Research Technology and Higher Education through the Basic Research Scheme. Number 345-08/UN7.D2/PP/IV/2023

References

Aani, S.A., Mustafa, T.N. & Hilal, N. 2020. Ultrafiltration membranes for wastewater and water process engineering: A comprehensive statistical review over the past decade. *J. Water Process Eng.*, 35: 101241. https://doi.org/10.1016/j.jwpe.2020.101241

Ahmed, M., Mavukkandy, M.O., Giwa, A., Elektorowicz, M., Katsou, E., Khelifi, O. & Hasan, S.W. 2022. Recent developments in the removal of hazardous pollutants from wastewater and water reuse within a circular economy. *NPJ Clean Water*, 5(1): 54. https://doi.org/10.1038/s41545-022-00154-5

Alam, R., Mahmood, R.A., Islam, S., Ardiati, F.C., Solihat, N.N., Alam, M.B. & Kim, S. 2022. Understanding the biodegradation pathways of azo dyes by immobilized white-rot fungus *Trametes hirsuta* D7 using UPLC-PDA-FTICR MS, supported by in silico simulations and toxicity assessment. *Chemosphere*, 313: 137505. https://doi.org/10.1016/j.chemosphere.2022.137505

Ayilara, M., Olanrewaju, O., Babalola, O. & Odeyemi, O. 2020. Waste management through composting: Challenges and potential. *Sustainability*, 12(11): 4456. https://doi.org/10.3390/su12114456

Bahry, M.S., Radjasa, O.K. & Trianto, A. 2021. Potential of marine sponge-derived fungi in aquaculture. *Biodiversitas J. Biol. Divers.*, 22(7): 1-8. https://doi.org/10.13057/biodiv/d220740

Barnett, H.L. & Hunter, B.B., 1972. Illustrated genera of imperfect fungi. 3rd ed, v+241 pp.

Caguiat, J.M.E., Tiu, E.R.U., Go, A.D., Rosa, F.M.D. & Punzalan, E.R. 2024. Dataset on the Decolorization of Naphthol Green B using a UV/sulfite system: optimization by response surface methodology. *Data Brief*, 57: 110924. https://doi.org/10.1016/j.dib.2024.110924

Wang, C.-Y., Kong, X.-W. & Liu, C. 2017. Process color watermarking: The use of visual masking and dot gain correction. *Multimed. Tools Appl.*, 76(15): 16291–16314. https://doi.org/10.1007/s11042-016-3909-x

Cemalgil, S., Onat, O., Tanaydın, M.K. & Etli, S., 2021. Effect of waste textile dye adsorbed almond shell on self compacting mortar. *Constr. Build. Mater.*, 300:123978. https://doi.org/10.1016/j.conbuildmat.2021.123978

Chin, J.M.W., Puchooa, D., Bahorun, T. & Jeewon, R. 2021. Antimicrobial properties of marine fungi isolated from sponges and brown algae of Mauritius. *Mycology*, 12(4): 231–244. https://doi.org/10.1080/21501203.2021.1895347

Danish, M., Khanday, W.A., Hashim, R., Sulaiman, N.S.B., Akhtar, M.N. & Nizami, M., 2017. Application of optimized large surface area date stone (*Phoenix dactylifera*) activated carbon for rhodamin B removal from aqueous solution: Box-Behnken design approach. *Ecotoxicol. Environ. Saf.*, 139: 280–290. https://doi.org/10.1016/j.ecoenv.2017.02.001

De Paula, N.M., da Silva, K., Brugnari, T., Haminiuk, C.W.I. & Maciel, G.M., 2022. Biotechnological potential of fungi from a mangrove ecosystem: Enzymes, salt tolerance, and decolorization of a real textile effluent. *Microbiol. Res.*, 254: 126899. https://doi.org/10.1016/j.micres.2021.126899

Franciscon, E., Grossman, M.J., Paschoal, J.A.R., Reyes, F.G.R. & Durrant, L.R., 2012. Decolorization and biodegradation of reactive sulfonated azo dyes by a newly isolated *Brevibacterium* sp. strain VN-15. *Springerplus*, 1(1):1–10. https://doi.org/10. 1186/2193-1801-1-37

Géry, A., Delanoe, A., Heutte, N., Chosson, E., Bonhomme, J. & Garon, D., 2021. A novel qPCR based-method for detection and quantification of three recurrent species of Penicillium isolated from bioaerosols in fungi-damaged homes. *J. Microbiol. Methods*, 186: 106236. https://doi.org/10.1016/j.mimet. 2021.106236

Gobalakrishnan, R. & Bhuvaneswari, R. 2019. Microbial fuel cells potential of marine actinobacteria *Actinoalloteichus* sp. MHA15 from the Havelock island of the Andamans, India. *Biotechnol. Res. Innov.*, 3(1): 144–158. https://doi.org/10.1016/j.biori.2019.01.003

Haris, A., Mouchtari, M.E. & Nurshofia, V. 2024. Polycyclic Aromatic Hydrocarbons (PAHs) potential sources in sediments of Plawangan Timur, Segara Anakan, Cilacap: Occurrence and distribution. *Ilmu Kelautan Indonesian Journal of Marine Science*, 29(1): 1-10. https://doi.org/10.14710/ik.ijms.29.1.1-10

He, X., Song, C., Li, Y., Wang, N., Xu, L., Han, X. & Wei, D. 2018. Efficient degradation of Azo dyes by a newly isolated fungus *Trichoderma tomentosum* under non-sterile conditions. *Ecotoxicol. Environ. Saf.*, 150: 232–239. https://doi.org/10.1016/j.ecoenv.2017.12.043

Hong, Y., Guo, M. & Wang, J. 2021. ENJ algorithm can construct triple phylogenetic trees. *Mol. Ther. Nucleic Acids*, 23: 286–293. https://doi.org/10.1016/j.omtn.2020.11.004

Hossen, M.Z., Hussain, M.E., Hakim, A., Islam, K., Uddin, M.N. & Azad, A.K., 2019. Biodegradation of reactive textile dye Novacron Super Black G by free cells of newly isolated *Alcaligenes faecalis* AZ26 and *Bacillus* spp obtained from textile effluents. *Heliyon*, 5(7): e02068. https://doi.org/10.1016/j.heliyon.2019.e02 68

Jefri, P., Respati, T.S., Sabirin, M., Meta, P.P., Zulfa, A. & Lukas, P. 2021. Antimalarial Activity of Sea Sponge Extract of *Stylissa massa* originating from waters of Rote Island. *J. Kim. Sains Aplikas J. Sci. Appl. Chem.*, 24(4): 136–145. https://doi.org/10.14710/jksa.24.4.136-145

Jing, M., Han, G., Li, Y., Zong, W. and Liu, R. 2022. Cellular and molecular responses of earthworm coelomocytes and antioxidant enzymes to naphthalene and a major metabolite (1-naphthol). *J. Mol. Liq.*, 350: 118563. https://doi.org/10.1016/j.molliq.2022.118563

Lalnunhlimi, S. & Veenagayathri, K. 2016.

Decolorization of azo dyes (Direct Blue 151 and Direct Red 31) by moderately alkaliphilic bacterial consortium. *Braz. J. Microbiol.*, 47(1): 39–46. https://doi.org/10.1016/j.bjm.2015.11.013

Lellis, B., Fávaro-Polonio, C.Z., Pamphile, J.A. & Polonio, J.C. 2019. Effects of textile dyes on health and the environment and bioremediation potential of living organisms. *Biotechnol. Res. Innov.*, 3(2): 275–290. https://doi.org/10.1016/j.biori.2019.09.001

Madalosso, H.B., de Castro Santos, B., Ribeiro, L.F.B., Machado, R.A.F. & Marangoni, C., 2022. Improvement of Membrane Hydrophobicity by One-Step Electrospraying for Water Recovery from Textile Dye Solution by Membrane Distillation. *SSRN Electron. J.*, 165: 357–373. https://doi.org/10.2139/ssrn.3972673

Maharsiwi, W., Astuti, R.I., Meryandini, A. & Wahyudi, A.T., 2020. Screening and characterization of sponge-associated bacteria from Seribu Island, Indonesia producing cellulase and laccase enzymes. *Biodiversitas*, 21(3): 975–981. https://doi.org/10.13057/bio div/d210317

Ndive, J.N., Eze, S.O., Nnabuife, S.G., Kuang, B. & Rana, Z.A. 2024. Dual-Chamber microbial fuel cell for Azo-Dye degradation and electricity generation in Textile wastewater treatment. *Waste Manag. Bull.*, 3(3): 100195:. https://doi.org/10.1016/j.wmb.2025.100195

Phuangsaijai, N., Jakmunee, J. & Kittiwachana, S. 2021. Investigation into the predictive performance of colorimetric sensor strips using RGB, CMYK, HSV, and CIELAB coupled with various data preprocessing methods: A case study on an analysis of water quality parameters. *J. Anal. Sci. Technol.*, 12(1): 1–16. https://doi.org/10.1186/s40543-021-00271-9

Riesco, R., Carro, L., Román-Ponce, B., Prieto, C., Blom, J., Klenk, H. & Trujillo, M.E. 2018. Defining the Species *Micromonospora saelicesensis* and *Micromonospora noduli* Under the Framework of Genomics. *Front. Microbiol.*, 9: 1360. https://doi. org/10.3389/fmicb.2018.01360

Schmidt, C., Berghahn, E., Ilha, V. & Granada, C.E. 2019. Biodegradation potential of Citrobacter cultures for the removal of amaranth and congo red azo dyes. *Int. J. Environ. Sci. Technol.*, 16(11): 6863–6872. https://doi.org/ 10.1007/s13762-019-02274-x

Shintianata, D., Lubis, A.A., Sugiharto, U. & Amalia, R. 2024. Tracing heavy metal dynamics in mangrove sediments: A study from Ujung Kulon National Park. *Ilmu Kelautan Indonesian Journal Marine Science*, 29(4): 519-529. https://doi.org/10. 14710/ik.ijms.29.4.519-529

Sibero, M., Ocky, K., Sabdono, A., Trianto, A., Triningsih, D. & Hutagaol, I. 2018. Antibacterial activity of Indonesian sponge associated fungi against clinical pathogenic multidrug resistant bacteria. *J. Appl. Pharm. Sci.*, 8(2): 088-094. https://doi.org/10.7324/japs.2018.8214

Srinivasan, S. & Sadasivam, S.K. 2021. Biodegradation of textile azo dyes by textile effluent non-adapted and adapted *Aeromonas hydrophila*. *Environ. Res.*, 194: 110643. https://doi.org/10.1016/j.envres.2020.110643

Sukardi, R.W., Djawad, M.I., Azis, H.Y. & Manaf, S.R. 2024. Impact of varied lead concentrations on accumulation and gill damage of milkfish (*Chanos chanos*). *Ilmu Kelautan Indonesian. Journal of Marine Science*, 29(1): 85-96. https://doi.org/10.14710/ik.ijms.29.1.85-96

Torres-Garcia, D., Gene, J. & Garcia, D. 2022. New and interesting species of Penicillium (Eurotiomycetes, Aspergillaceae) in freshwater sediments from Spain. *MycoKeys*, 86: 103–145. https://doi.org/10.3897/mycokeys.86.73861

Trianto, A., Radjasa, O.K., Sibero, M.T., Sabdono, A., Haryanti, D.W.I., Zilullah, W.O.M., Syanindyta, A.R., Bahry, M.S., Widiananto, P.A., Helmi, M. & Armono, H.D. 2020. The effect of culture media on the number and bioactivity of marine invertebrates associated fungi. *Biodiversitas*, 21(1): 407–412. https://doi.org/10.13057/biodiv/d210147

Trianto, A., Radjasa, O.K., Subagiyo, S., Isabella, A.A., Bahry, M.S., Purnaweni, H., Djamaludin, R., Tjoa, A., Singleton, I., Evans, D.M. & Diele, K. 2023. Molecular Identification and Biotechnological Potential of Cerithidea cingulata- and Lottia scabra Associated Fungi as Extracellular Enzyme Producer and Anti-Vibriosis Agent. *Ilmu Kelautan Indonesian Journal of Marine Science*, 28(2): 136–147. https://doi.org/10.14710/ik.ijms.28.2.136-147

Tsamo, C., Kidwang, G.D. & Dahaina, D.C. 2020. Removal of Rhodamine B from aqueous solution using silica extracted from rice husk. *SN Appl.*

Sci., 2(2): 1–13. https://doi.org/10.1007/s42452-020-2057-0

Zakariya, N.A., Majeed, S. & Jusof, W.H.W. 2022. Investigation of antioxidant and antibacterial activity of iron oxide nanoparticles (IONPS) synthesized from the aqueous extract of *Penicillium* spp. *Sensors Int.*, 3: 100. https://doi.org/10.1016/j.sintl.2022.100